NURETH14-396

DETERMINING TEMPERATURE AND STRESS DISTRIBUTIONS IN PRESSURE COMPONENTS BASED ON MEASUREMENTS OF INTERNAL PRESSURE AND TEMPERATURE AT THE OUTER EASILY ACCESSIBLE SURFACE

J. Taler¹, B. Węglowski¹, T. Sobota¹, M. Jaremkiewicz¹, D. Taler²

¹ Cracow University of Technology, Cracow, Poland

² University of Science and Technology, Cracow, Poland
taler@mech.pk.edu.pl, weglowski@mech.pk.edu.pl, tsobota@mech.pk.edu.pl,
mjaremkiewicz@pk.edu.pl, taler@imir.agh.edu.pl

Abstract

A method for monitoring transient thermal stresses based on the solution of the inverse heat conduction problem is presented. Thermal stresses are determined indirectly on the basis of measured temperature values taken at selected points on the outer surface of a pressure element. First, transient temperature distribution in the whole pressure component is calculated, subsequently thermal stresses are determined using the finite element method. Measured pressure changes are used to calculate internal-pressure caused stresses. Next, the results of temperature and stress monitoring in the thick walled pipe are presented and compared with experimental data. Very good coincidence was found between computational and experimental results.

Introduction

Thermal stresses can limit the heating and cooling rates of temperature changes. The largest absolute value of thermal stresses appears at the inner surface. Direct measurements of these stresses are very difficult to take, since the inner surface is in contact with water or steam under high pressure. For that reason, thermal stresses are calculated in an indirect way based on measured temperatures at selected points, located on an outer thermally insulated surface of a pressure element. First, time-space temperature distribution in pressure element is determined using the inverse space marching method.

High thermal stresses often occur in partially filled horizontal vessels. During operation under transient conditions, for example, during power plant start-up and shut-down, there are significant temperature differences over the circumference of the horizontal pressure vessels [1, 2]. This phenomenon is caused by the different heat transfer coefficients in the water and steam spaces. This takes place in large steam generator drums, superheater headers and steam pipelines. High thermal stresses caused by nonuniform temperature distribution on vessel circumference also occur in emergency situations such as fire of partially filled fuel tanks. The upper part of the horizontal vessel is heated much faster than the lower part filled with liquid.

Similar phenomenon occurs in inlet nozzles in PWR nuclear reactor, at which high temperature differences on the circumference of the feed water nozzles are observed.

The study presents an analysis of transient temperature and stress distribution in a cylindrical pressure component during start-up of the steam boiler and shut-down operations. Thermal stresses are determined indirectly on the basis of measured temperature values at selected points on the outer surface of a pressure element. Heaving determined transient temperature distribution in the entire component, thermal stresses are determined using the finite element method. Measured pressure changes are used to calculate pressure caused stresses. The calculated temperature histories were compared with the experimental data at selected interior points.

The presented method of thermal stress control was applied in a few large conventional power plants. It can also be used successfully in nuclear power plants. The developed method for monitoring thermal stresses and pressure-caused stresses is also suitable for nuclear power plants, since it does not require drilling holes for sensors in pressure element walls. Measurements conducted over the last few years in power plants demonstrate that the presented method of stress monitoring can be applied in systems for controlling boiler start-up operations and in systems for monitoring the fatigue and creep usage factor of pressure components.

1. Present methods used to determine temperature and thermal stress transient in boiler pressure elements

The simplest and most frequently used method for reducing thermal stresses in pressure elements is to limit heating and cooling rates. The allowable rates of fluid temperature changes can be determined using German Boiler Codes TRD 301 [3] or European Standard EN 12952-3 [4]. The allowable heating rate of temperature changes is determined from the following condition [3, 4]

$$\alpha_m \frac{\left(p - p_o\right) d_m}{2s} + \alpha_T \phi_w \phi_f \frac{v_T s^2}{a} = \sigma_{\min}.$$
 (1)

The maximum allowable cooling rate is calculated in a similar way:

$$\alpha_m \frac{(p - p_o)d_m}{2s} + \alpha_T \phi_w \phi_f \frac{v_T s^2}{a} = \sigma_{\text{max}}.$$
 (2)

In equations (1-2), the following nomenclature is used: $\alpha = k/(c \cdot \rho)$ – thermal diffusivity, m²/s, $d_m = r_{out} + r_{in}$ – mean diameter, m, p – absolute pressure, MPa, p_o – ambient pressure, MPa, $s = r_{out} - r_{in}$ – thickness of cylindrical element, m, v_T – rate of temperature changes of fluid or pressure element wall, K/s, α_m – pressure caused stress intensity factor, α_T – thermal stress intensity factor, σ_{min} – allowable stress during shutdown (cooling), MPa.

Coefficients ϕ_w and ϕ_f are defined as follows

$$\phi_{w} = \frac{E\beta}{1 - \nu},\tag{3}$$

$$\phi_f = \frac{(3u^2 - 1)(u^2 - 1) - 4u^4 \ln u}{8(u^2 - 1)(u - 1)^2},$$
(4)

where: E – Young's modulus, MPa, β – linear coefficient of thermal expansion, 1/K, ν – Poisson ratio, $u = r_{out}/r_{in}$ – ratio of outer to inner surface radius.

Equations (1-2) can also be used to calculate the maximum total stress at hole edges. The heating or cooling rate of temperature changes in pressure elements v_T can be calculated using the moving average filter [5]

$$v_{T} = \frac{df}{dt}\Big|_{t=t_{i}} = \frac{1}{693\Delta t} \left(-63f_{i-4} + 42f_{i-3} + 117f_{i-2} + 162f_{i-1} + 177f_{0} + 162f_{i+1} + 117f_{i+2} + 42f_{i+3} - 63f_{i+4} \right),$$
(5)

where f_i are medium or wall temperatures at nine successive time points with Δt time step.

Equations (1-2) and (5) are not only valid for a quasi-steady state [5], but also when the temperature change rate v_T is the function of time: $v_T = v_T(t)$. For pressure components with complex geometry, the stress value in the stress concentration areas can be calculated using the finite element method (FEM). By determining the so called influence function with the use of the FEM, one is subsequently able to carry out an on-line stress calculation with known heat transfer coefficient and fluid temperature transient [6].

This paper formulates the problem of determining the transient temperature in a pressure element as an inverse transient heat conduction problem. The temperature distribution is determined on the basis of temperature histories measured at selected points at the outer insulated surface of a pressure component. After determining transient temperature distribution in the entire pressure component, thermal stresses are computed using the FEM. Inverse problem is solved using the finite volume method (FVM). Thermal and pressure caused stresses are calculated using the FEM.

2. Mathematical formulation of the problem

In the following, two dimensional inverse heat conduction problem will be solved (Fig. 1). The analyzed domain is divided into two subdomains: direct and inverse. Boundary and initial conditions are known for the direct region so that the transient temperature distribution is obtained for the solution of the boundary-initial problem. The temperature distribution on the inner closed surface S_m which is located inside the analyzed area (Fig. 1) is known from measurements. Based on the solution of the direct problem the heat flux on the boundary S_m can be evaluated. Thus, the two boundary conditions are known on the surface S_m :

$$T(s,t)\Big|_{S_{-}} = f(s,t), \tag{6}$$

$$-k\frac{\partial T}{\partial n}\bigg|_{S} = q(s,t),\tag{7}$$

while on the inner surface S_{in} of the body, the temperature and heat flux are unknown.

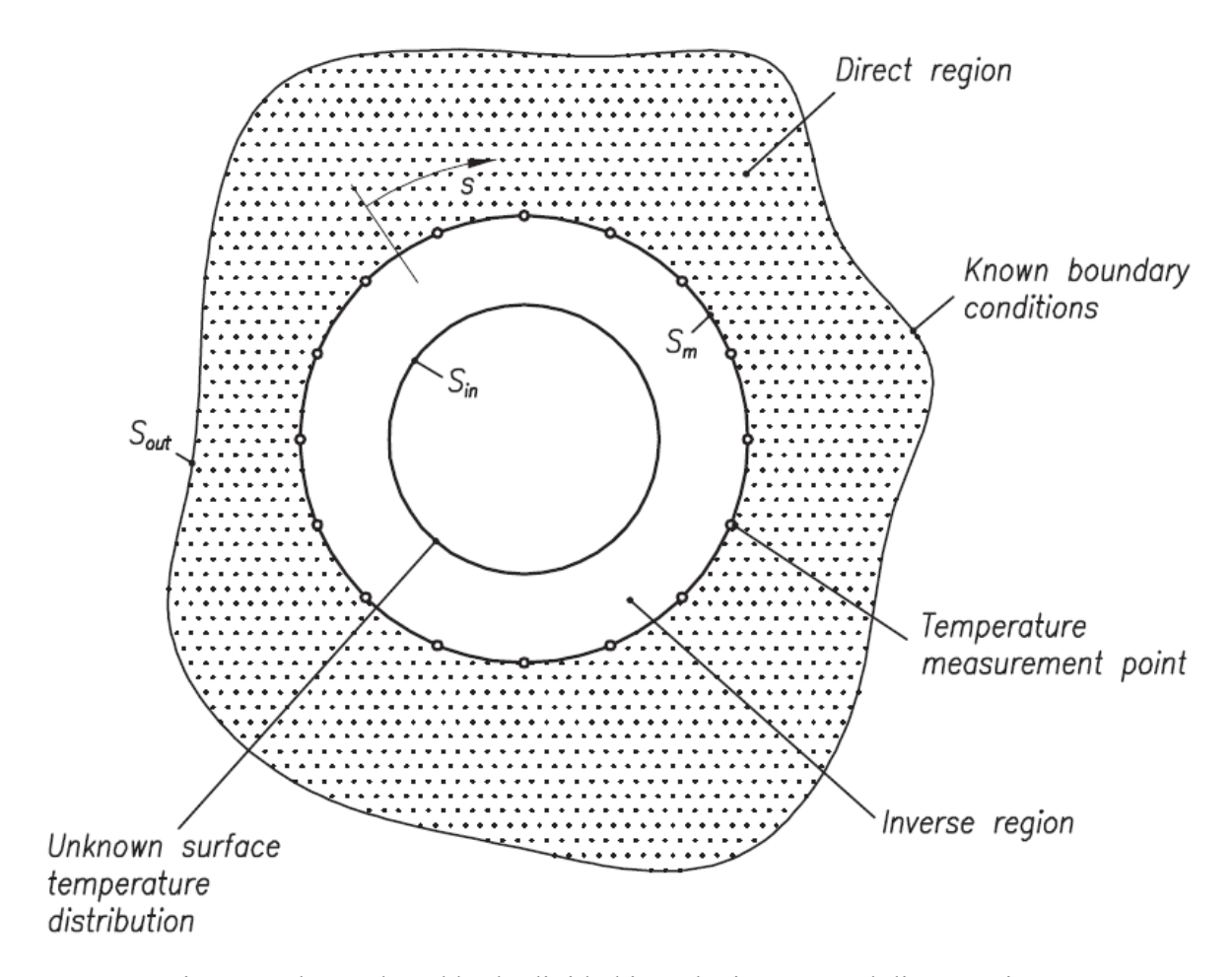


Figure 1 The analyzed body divided into the inverse and direct regions

In order to evaluate the transient temperature distribution in the inverse region, this region is divided into control volumes (Fig. 2). The method marches in space towards the inner body surface S_{in} by using the energy balance equations for the finite volumes placed on the boundary S_m to determine the temperatures in adjacent nodes. In this way of proceeding the time derivatives of the measured temperature changes have to be calculated. The accurate calculation of the time derivatives of the measured temperature histories is difficult since the measured temperature values are burdened with random measurement errors. Thus, time-temperature charts have to be smoothed before evaluating the time derivative. In the present paper this was achieved by using the local polynomial approximation. The successive nine temperature data points were approximated using the polynomial of the 3rd degree and then the derivatives in the middle of each interval (time coordinate of the point 5) were calculated.

The space-marching method will be illustrated by an example showing the evaluation of the temperature distribution in the cylindrical wall using the temperature measurement points equally distributed on the surface S_m (Fig. 2). It is assumed that the temperature and heat flux distributions are known on the surface S_m from temperature measurements at points 16-22 and from the solution of the direct problem.

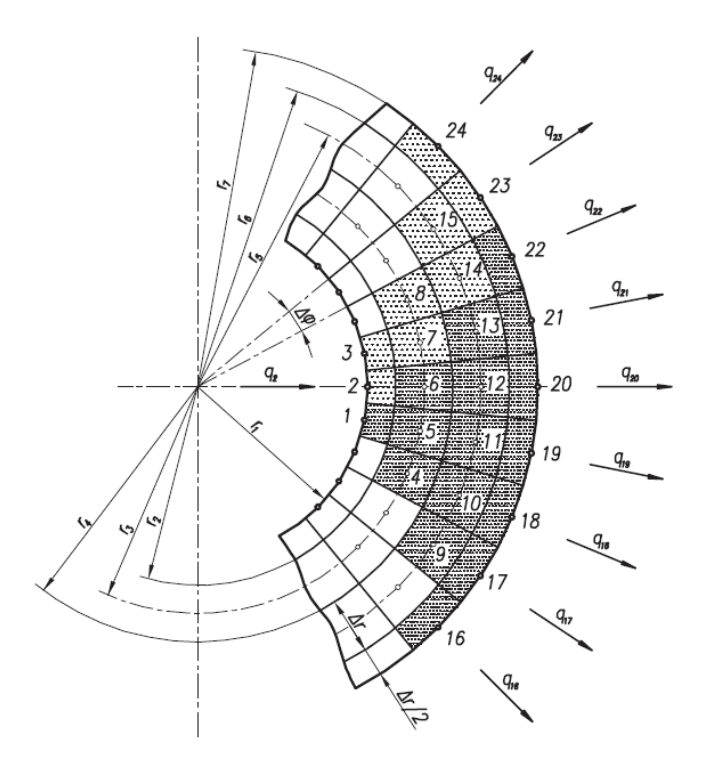


Figure 2 Division of the inverse region into control volumes

For the ideally insulated outer surface the heat fluxes q_{16} - q_{22} and their time derivatives are equal to zero. At first, the discrete energy conservation equations are set for the control volumes. The energy balance equation for the finite volume with the node (i, j) is as follows (Fig. 3):

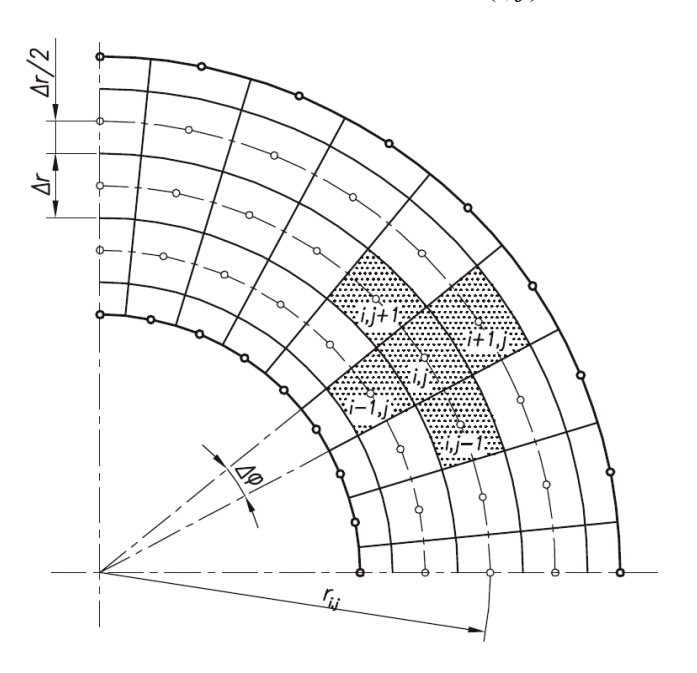


Figure 3 Space marching in the inverse region

$$\frac{1}{2} \left[\left(r_{i,j} + \frac{\Delta r}{2} \right)^{2} - \left(r_{i,j} - \frac{\Delta r}{2} \right)^{2} \right] \Delta \varphi \, c \left(T_{i,j} \right) \rho \left(T_{i,j} \right) \frac{dT_{i,j}}{dt} =$$

$$= \left(r_{i,j} + \frac{\Delta r}{2} \right) \Delta \varphi \, \frac{k \left(T_{i,j} \right) + k \left(T_{i+1,j} \right) T_{i+1,j} - T_{i,j}}{2} +$$

$$+ \left(r_{i,j} - \frac{\Delta r}{2} \right) \Delta \varphi \, \frac{k \left(T_{i,j} \right) + k \left(T_{i-1,j} \right) T_{i-1,j} - T_{i,j}}{2} + \Delta r \, \frac{k \left(T_{i,j+1} \right) + k \left(T_{i,j} \right) T_{i,j+1} - T_{i,j}}{2} +$$

$$+ \Delta r \, \frac{k \left(T_{i,j-1} \right) + k \left(T_{i,j} \right) T_{i,j-1} - T_{i,j}}{2} , \tag{8}$$

where: c – specific heat, J/(kg·K); ρ – density, kg/m³; k – thermal conductivity, W/(m·K); t – time, s; T – temperature, °C; Δr – space step in radial direction, m; $\Delta \varphi$ – angular step, rad (Fig. 3).

Transforming the heat balance Equation (8) for $T_{i-1,j}$, we obtain:

$$T_{i-1,j} = T_{i,j} + \Delta r \frac{\left(r_{i,j} + \frac{\Delta r}{2}\right)^{2} - \left(r_{i,j} - \frac{\Delta r}{2}\right)^{2}}{r_{i,j} - \frac{\Delta r}{2}} \cdot \frac{c\left(T_{i,j}\right)\rho\left(T_{i,j}\right)}{k\left(T_{i,j}\right) + k\left(T_{i-1,j}\right)} \cdot \frac{dT_{i,j}}{dt} - \frac{-\frac{\Delta r}{2}}{r_{i,j} - \frac{\Delta r}{2}} \cdot \frac{k\left(T_{i,j}\right) + k\left(T_{i+1,j}\right)}{k\left(T_{i,j}\right) + k\left(T_{i-1,j}\right)} \cdot \left(T_{i+1,j} - T_{i,j}\right) - \frac{\left(\Delta r\right)^{2}}{r_{i,j} - \frac{\Delta r}{2}} \cdot \frac{k\left(T_{i,j+1}\right) + k\left(T_{i,j}\right)}{k\left(T_{i,j}\right) + k\left(T_{i-1,j}\right)} \cdot \frac{T_{i,j+1} - T_{i,j}}{\Delta \varphi^{2} r_{i,j}} - \frac{\left(\Delta r\right)^{2}}{r_{i,j} - \frac{\Delta r}{2}} \cdot \frac{k\left(T_{i,j-1}\right) + k\left(T_{i,j}\right)}{k\left(T_{i,j}\right) + k\left(T_{i-1,j}\right)} \cdot \frac{T_{i,j-1} - T_{i,j}}{\Delta \varphi^{2} r_{i,j}}.$$

$$(9)$$

Since Eq. (9) is nonlinear, the fixed-point iterative technique is used to determine the temperature $T_{i,j-1}$:

$$T_{i-1,j}^{(n+1)} = T_{i,j} + \Delta r \frac{\left(r_{i,j} + \frac{\Delta r}{2}\right)^{2} - \left(r_{i,j} - \frac{\Delta r}{2}\right)^{2}}{r_{i,j} - \frac{\Delta r}{2}} \frac{c\left(T_{i,j}\right)\rho\left(T_{i,j}\right)}{k\left(T_{i,j}\right) + k\left(T_{i-1,j}^{(n)}\right)} \frac{dT_{i,j}}{dt} - \frac{r_{i,j} + \frac{\Delta r}{2}}{k\left(T_{i,j}\right) + k\left(T_{i+1,j}\right)} \left(T_{i+1,j} - T_{i,j}\right) - \frac{\left(\Delta r\right)^{2}}{r_{i,j} - \frac{\Delta r}{2}} \frac{k\left(T_{i,j+1}\right) + k\left(T_{i,j}\right)}{k\left(T_{i-1,j}\right)} \frac{T_{i,j+1} - T_{i,j}}{\Delta \varphi^{2} r_{i,j}} - \frac{\left(\Delta r\right)^{2}}{r_{i,j} - \frac{\Delta r}{2}} \frac{k\left(T_{i,j+1}\right) + k\left(T_{i-1,j}\right)}{\left(T_{i,j}\right) + k\left(T_{i-1,j}\right)} \frac{T_{i,j-1} - T_{i,j}}{\Delta \varphi^{2} r_{i,j}}.$$

$$(10)$$

The iteration process continuous until the condition $\left|T_{i-1,j}^{(n+1)} - T_{i-1,j}^{(n)}\right| \le \varepsilon$ is satisfied. Symbol *n* denotes the iteration number and ε is some small number (tolerance), for example, $\varepsilon = 0.0001$ K. If the thermal properties are constant, the iterations are not required.

To determine the wall temperature at the node 1 (Fig. 2) we proceed as follows. First the heat balance equations are written for the nodes 16 to 22 from which the temperature at the nodes 9 to 13 is determined. Then the heat balance equations are set for the nodes 9 to 13 from which the temperature at the nodes 4 to 6 is evaluated. From the heat equations for the nodes 4, 5 and 6, we can determine the temperature at node 1 located at the inner surface of the pressure component. Based on the measured temperatures at the nodes 17 to 23, the temperature at the node 2 is calculated in similar way. Using the measured temperature at nodes 18 to 24 the temperature at the node 3 is estimated.

Repeating the procedure described above for all the nodes, located at the outer surface, at which the wall temperature is measured, the temperature at the nodes situated at the inner component surface are determined. After determining the temperature distribution at the whole cross-section at the time point t, the temperature distribution at time $t + \Delta t$ is computed. After calculating the temperature distribution the thermal stresses were calculating using the FEM. The finite element mesh is constructed so that the FEM nodes are coincident with the nodes used in the finite volume method

Random measurement errors of the temperature $f_j(t)$ have great influence on the estimated temperature and thermal stress distributions. If the temperature data are burdened with random errors, least squares smoothing is used to reduce the effect of the measurement errors on the calculated time derivatives df_j/dt or $dT_{i,j}/dt$. The Gram orthogonal polynomials were used for smoothing the measured time-temperature history $f_i(t)$ and estimated temperatures $T_{i+1,j}(t)$ [5].

3. Experimental validation of the developed method

In order to validate the developed method and to improve the computer system for continuous monitoring the power boiler operation, modern experimental installation was built. During its construction, particular emphasis was placed on ensuring that the conditions are similar to those that may occur in pressure components installed in power plants. In addition to metal temperature, temperature, mass flow rate, and pressure of the steam were measured as a function of time. To measure temperature distribution on the outer surface of the steam header precalibrated thermocouples were used. The experimental installation consists of the following elements:

- steam generation unit with steam output capacity 700 kg/h, equipped with a three-stage oil burner,
- installation for boiler feed water treatment,
- tray-type (cascade-type) deaerator,
- blow down flash-vessel for heat recovery,
- steam pressure reduction station 10 bar /4 bar /2 bar,
- boiler control system,
- steam header (horizontal pipe) made of martensitic high alloy P91 steel.



Figure 4 View of the experimental installation for testing the computer system for on-line monitoring thick-wall pressure components

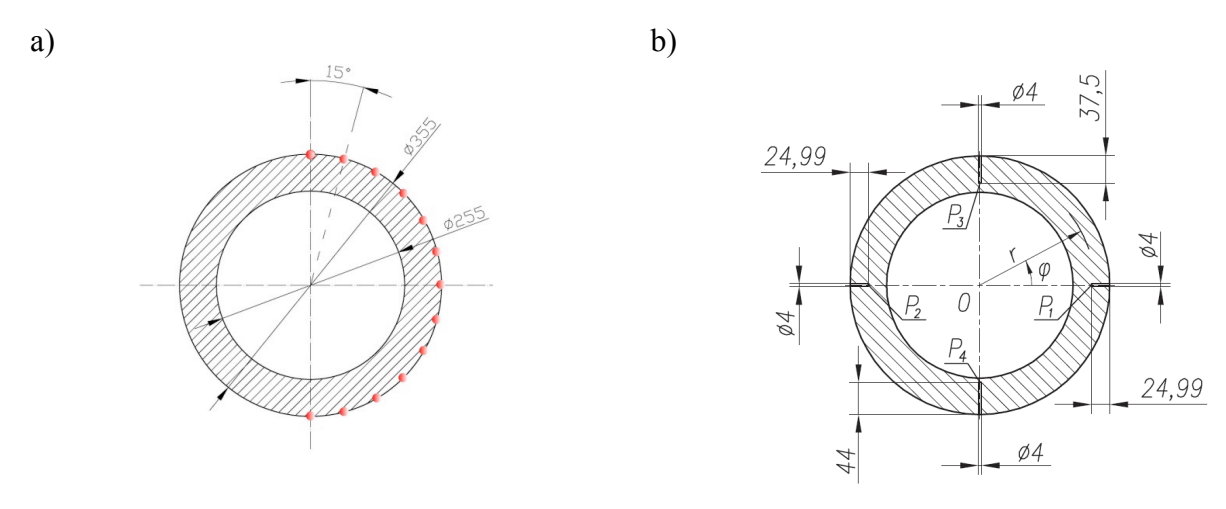


Figure 5 Location of temperature sensors on the steam header a) thermocouples at the outer surface of the steam header, b) location of interior thermocouples used for experimental validation of the inverse procedure

The measurements of temperature carried out on the outer surface of the steam header will be used for the determination of the temperature and stress distributions at the wall cross-section including the inner and outer surfaces of the steam header using the inverse heat conduction methods.

The steam header was made out of the martensitic high alloy P91 steel. The following physical properties of the P91 steel have been adopted for calculations: specific heat, c = 486 J/(kg·K),

thermal conductivity, k=29 W/(m·K), density, $\rho=7750$ kg/m³, modulus of elasticity, $E=2,28\cdot10^{11}$ Pa, Poissonn's ratio, v=0,29, coefficient of thermal expansion $\beta=0,098\cdot10^4$ 1/K. The outer diameter d_{out} , wall thickness δ and the length L are: 355 mm, 50 mm and 3765 mm, respectively. Thirteen thermocouples NiCr-NiAl (K-type) were mounted every 15° on the half of the outer circumference at the distance of 2150 mm from the inlet of steam (Fig. 5a). The actual temperatures measured at the outer surface of the steam header were used in the analysis. To validate the inverse technique developed in the paper, four thermocouples were installed at the interior locations: $\delta_I = \delta_2 = d_{out} - 0,50\delta$, $\delta_3 = d_{out} - 0,75\delta$ and $\delta_4 = d_{in} + 6$ mm (Fig. 5b), where the symbol δ denotes the tube thickness. These measurements were carried out with sheathed thermocouples NiCr-NiAl (K-type) with outer diameter of 3 mm. The temperatures measured at seven nodes 22-28 on the outer surface of the steam header (Fig. 6) were used for the determination of the temperature and stress distributions at the wall cross-section including the inner surface.

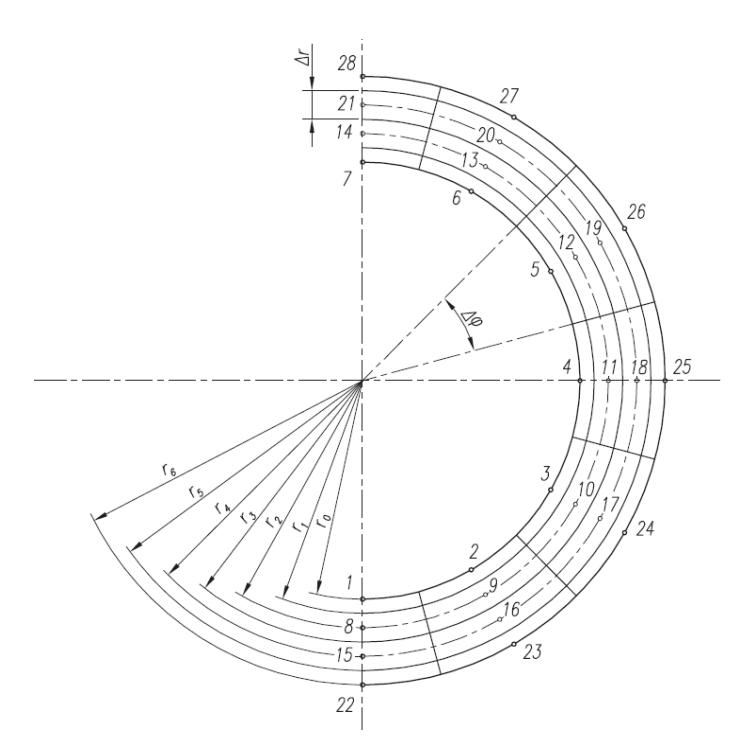


Figure 6 Division of the steam header cross-section into finite volumes

The agreement between the calculated and measured temperature values is satisfactory. The small discrepancies are caused by the delayed and damped response of the thermocouples.

The measured steam temperature, pressure and mass flow rate are depicted in Fig. 7a. The inspection of the results shown in Fig. 7a indicates that the fluid flow inside the tube is stratified. In the lower part of the header water is present, while through the upper part flows water steam. Calculated temperature histories are shown in Fig. 7b. The comparison of the calculated and measured temperature values at the interior points is shown in Fig. 8.

a) b)

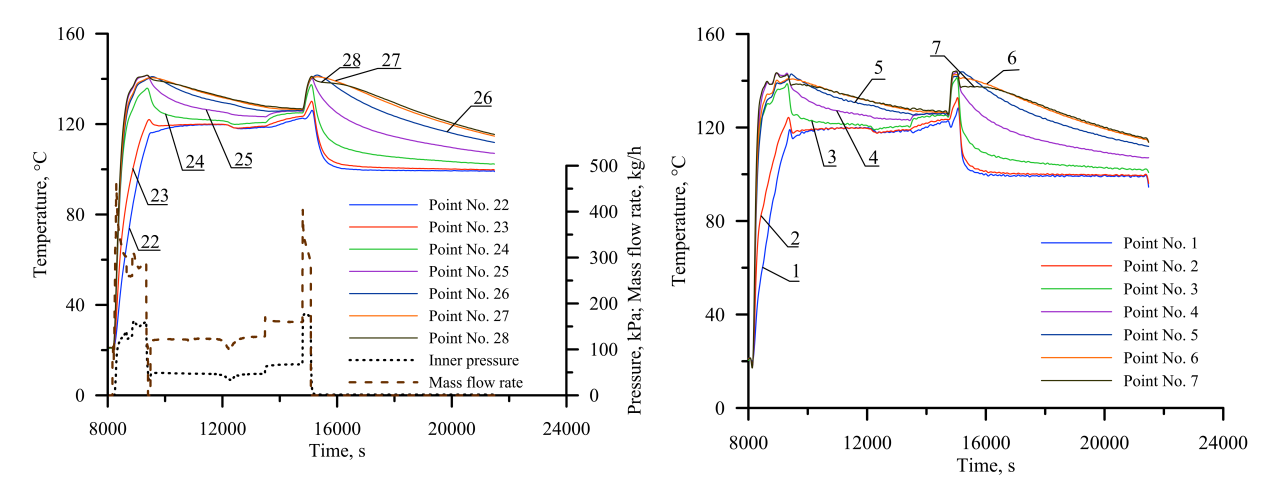


Figure 7 Time changes of the measured (a) and computed (b) temperature values

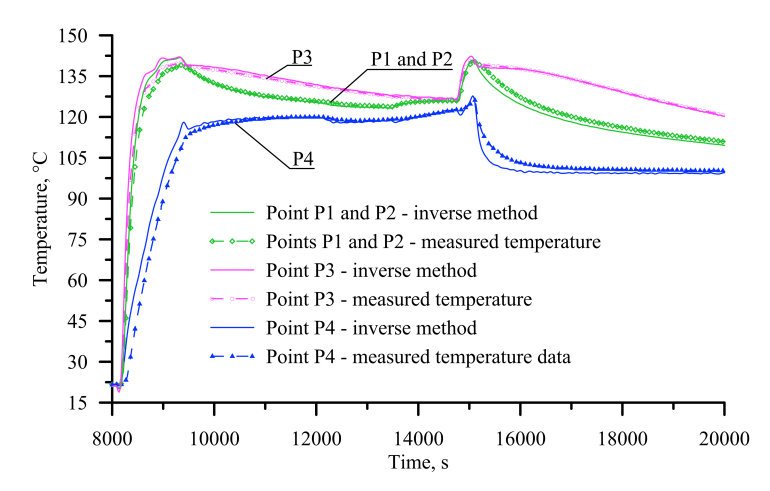


Figure 8 Comparison of the calculated and measured time changes of the wall temperature at the interior points

After determining the temperature distribution the thermal stresses and stresses due to inner pressure were calculated using the FEM. Circumferential and longitudinal stresses at the inner and outer header surfaces as functions of time are shown in Fig. 9 and 10, respectively. The sensitivity of the results obtained from the inverse analysis was investigated by adding random errors to the "exact" input temperatures which simulated measured temperatures at the outside surface of the header. The "exact measurement data" was artificially generated by solving direct heat conduction problem. The similar results were obtained for "exact data" and for temperatures burdened with random errors.

The largest stresses (Figs. 9-11) occur at the beginning of the heating process, when the ratio of wall temperature change is significant. The stresses at the outer surface are lower in comparison to the inner surface. The greatest absolute value has the longitudinal stress at the inner surface (Fig. 9-10). The stress components due to pressure are small in comparison with corresponding components of thermal stresses since the inner pressure during the test is very low (Fig. 7a).

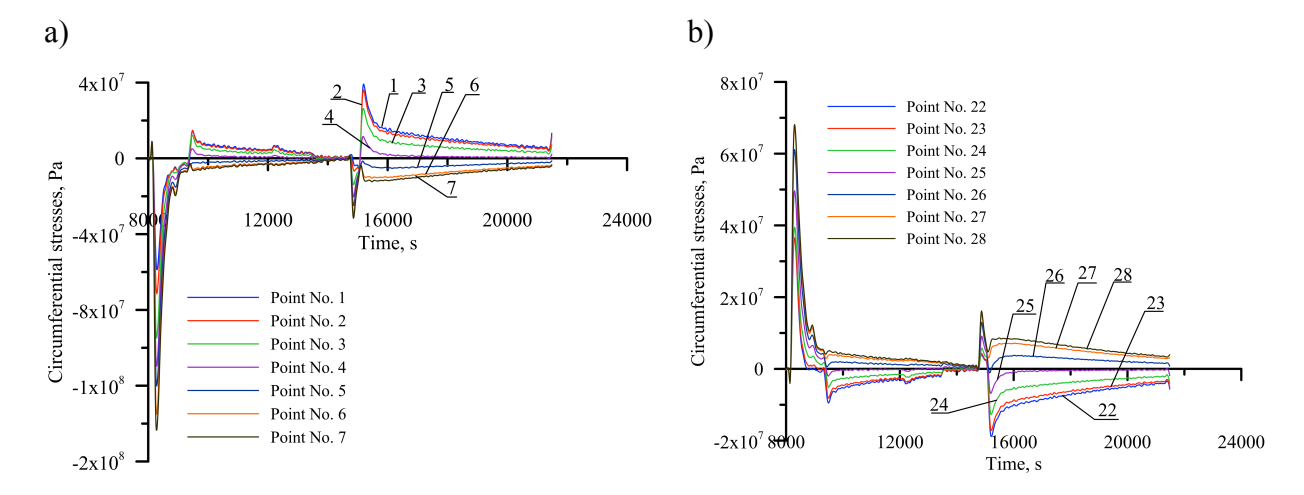


Figure 9 Circumferential stress as a function of time; (a) – inner surface, (b) – outer surface

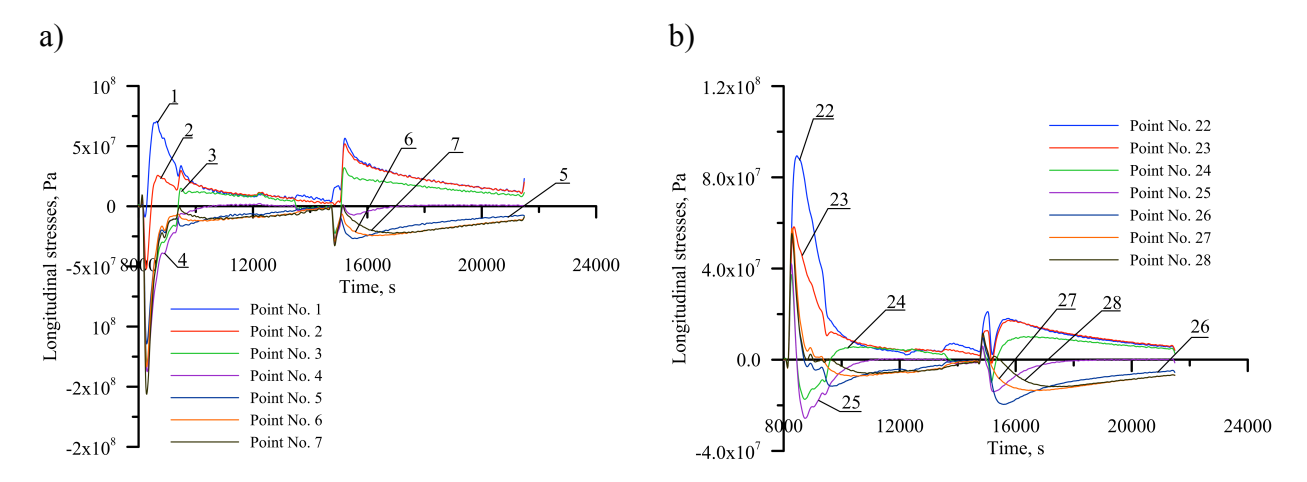


Figure 10 Longitudinal stress as a function of time; (a) – inner surface, (b) – outer surface

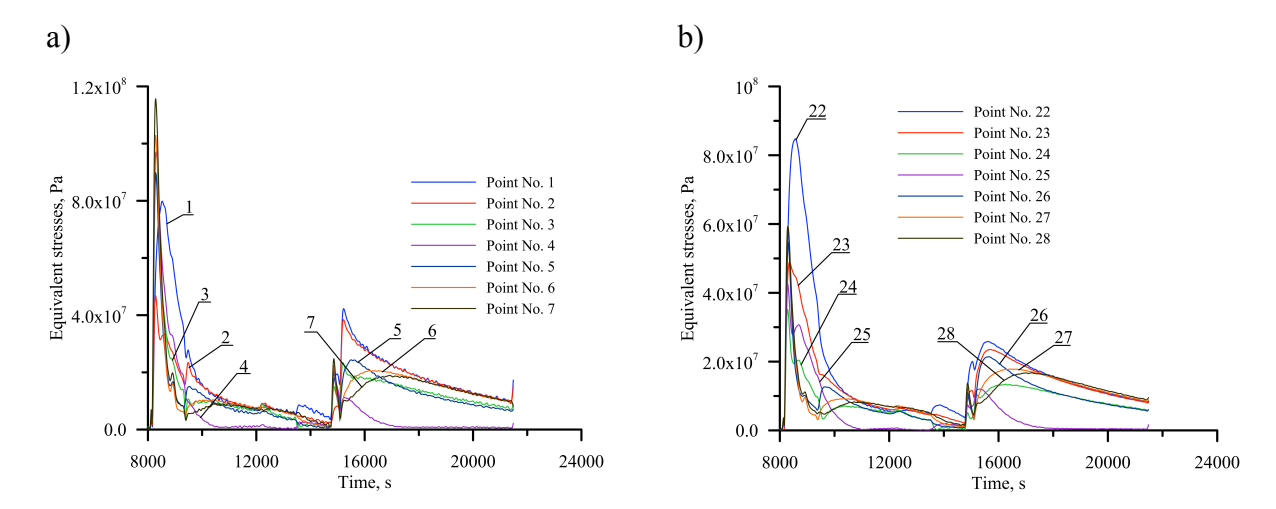


Figure 11 Equivalent stress as a function of time; (a) – inner surface, (b) – outer surface

4. Conclusions

The paper presents a method of transient temperature field identification in the drum on the basis of measured temperature changes at locations on the outer insulated surface of the pressure component. The method's accuracy was demonstrated by comparison of measured and calculated temperature at a few internal points. In order to reduce the sensitivity of the inverse method to random errors, the measured temperature histories were smoothed by the moving average filter based on the Gram's polynomials approximating nine successive measurement points. The smoothed value of measured temperature and its time derivatives are determined only in the middle of the interval, i.e., in time $t_i + 4(\Delta t)$, where t_i is time coordinate of the first point in the analyzed time interval: $[t_i, t_i + 8(\Delta t)]$. From the measured temperature histories on the outer surface of a pressure component, the temperature distribution can be determined at different time points in the whole cross section. Based on nodal temperatures determined in such a way, thermal stresses are calculated using FEM.

Values of fluid temperature and heat transfer coefficient on the inner surface of the component are not needed because the temperature distribution in the component cross section is determined by the developed method for solving the inverse heat conduction problem. Thus, the developed method is more accurate than the direct temperature distribution methods, because the fluid temperatures and heat transfer coefficients are unknown in operating components.

The method developed in the paper can be used for the stress identification in monitoring systems for the assessment of remnant lifetime of pressure components in conventional and nuclear power plants.

5. References

- [1] P. Rop, "DrumPlus: a drum type HRSG with Benson benefits", Modern Power Systems, Vol. 30, No. 10, 2010, pp. 35-40.
- [2] J.M. Fetköter, D.J. Lauer, M. Wedemeyer, G. Engelhard, "Replacement of Shutdown Cooling System and Repair of Nozzle Welds of Reactor Pressure Vessel in the Forsmark 1 + 2 Nuclear Power Plant", VGB PowerTech, No. 6, 2001, pp. 62-64.
- [3] TRD 301, Zylinderschalen unter innerem Überdruck. Technische Regeln für Dampfkessel (TRD), Heymanns Beuth Köln Berlin, S. 143-185, 2001.
- [4] European Standard EN 12952-3, "Water-tube boilers and auxiliary installations Part 3: Design and calculation for pressure parts", European Committee for Standardization, reu de Stassart, 36 B-1050 Brussels, 2001.
- [5] J. Taler, "Theory and Practice of Identification of Heat Transfer Processes", Ossolineum, Wrocław-Warszawa-Kraków, 1995, Poland (in Polish).
- [6] J. Taler, M. Zborowski, B. Węglowski, "Optimisation of Construction and Heating of Critical Structural Components of Boiler Drums, VGB PowerTech, Vol. 82, No. 11, 2002, pp. 19-24.